Journal of Ceramic Processing Research. Vol. 12, No. 4, pp. 435~438 (2011)

J O U R N A L O F
Ceramic Processing Research

Microwave-assisted synthesis of Ag incorporated $SrWO_4$/zeolite composites by a solid-state metathetic route

Won-Chun Oh, Jong Geun Choi, Chong Yeon Park and Chang Sung Lim*
Department of Advanced Materials Science & Engineering, Hanseo University, Seosan 356-706, Korea

A solid-state metathetic route assisted by a microwave irradiation was used to synthesize Ag incorporated $SrWO_4$/zeolite composites. The crystallized Ag incorporated $SrWO_4$/zeolite composites were formed at 600 °C for 3 h, showing a well immobilized morphology with particle sizes of 3-5 μm. The synthesized Ag incorporated $SrWO_4$/zeolite composites were characterized by scanning electron microscopy, energy-dispersive X-ray spectroscopy and Fourier transform infrared spectroscopy. The optical properties were investigated by photoluminescence emission and Raman spectroscopy.

Key words: Ag-$SrWO_4$/zeolite, Microwave-assisted, Solid-state metathetic synthesis, Luminescence, Raman spectroscopy.

Introduction

Metal tungstates have attracted considerable attention for potential applications in photoluminescence, scintillators, as photocatalyst and humidity sensors [1, 2]. The physical, chemical and photochemical properties of metal tungstates are dependent on the manufacturing method. Several processes have been developed over the past decade to enhance the applications of metal tungstates prepared by a range of processes, such as co-precipitation [3], a solvothermal method [4], spray pyrolysis [5], a reverse micelle system [6], solution synthesis [7], sol-gel [8], a mechano-chemical method [9], a molten salt method [10], a hydrothermal method [11], microwave-assisted synthesis [12] and solid-state metathetic reaction [13]. Wet chemical methods have disadvantages, such as complicated synthetic steps, use of expensive equipment, high synthesis temperatures and long sintering times. On the other hand, solid-state reactions require complex apparatus and techniques, which are becoming gradually unpopular due to the excessive energy consumption.

Compared with the usual methods, microwave synthesis has the advantages of a very short reaction time, a small particle size, a narrow particle size distribution, and a high purity method for preparing polycrystalline samples. Microwave heating is delivered to the surface of the material by radiant and/or convection heating, which is transferred to the bulk of the material via conduction. Microwave energy is delivered directly to the material through molecular interactions with an electromagnetic field. Heat can be generated through volumetric heating because microwaves can penetrate the material and supply energy [13]. Therefore it is possible to achieve rapid and uniform heating of thick materials. Solid-state synthesis of materials by the metathetic route is a simple and cost-effective method that provides a high yield with easy scale up, and is emerging as a viable alternative approach for the synthesis of high-quality novel inorganic materials in short time periods.

Ag incorporated $SrWO_4$/zeolite composites are expected to have excellent adsorption and synergy effects in an immobilization mechanism of metallic catalysts for a wide range of applications, such as sensors, photocatalysts, luminescence, anti-bacterial matrices, and optical effects in the UV and visible region. However, the study of microwave-assisted synthesis of Ag incorporated $SrWO_4$/zeolite composites by a solid-state metathetic (SSM) reaction has not been published previously. Therefore, the precise nature of the optical properties and microwave-assisted SSM synthesis of Ag incorporated $SrWO_4$/zeolite composites are required for a wide range of applications. In this study, Ag incorporated $SrWO_4$/zeolite composites were synthesized using a SSM method assisted by a microwave irradiation. The characteristics of the SSM reaction of Ag incorporated $SrWO_4$/zeolite composites are discussed in detail based on the formation of a high lattice energy by-product of NaCl. The synthesized Ag incorporated $SrWO_4$/zeolite composites were characterized by scanning electron microscopy (SEM), energy-dispersive X-ray spect- roscopy (EDS) and Fourier transform infrared spectroscopy (FTIR). The optical properties were examined by photoluminescence (PL) emission and Raman spectroscopy.

Experimental

$SrCl_2 \cdot 6H_2O$ and $Na_2WO_4 \cdot 2H_2O$ of analytic reagent grade were used to prepare the $SrWO_4$ compound. The preparation of $SrWO_4$ was carried out by reacting well-ground mixtures of $SrCl_2 \cdot 6H_2O$ and $Na_2WO_4 \cdot 2H_2O$ at a molar ratio of 1 : 1. The sample mixtures were dried at

*Corresponding author:
Tel : +82-41-660-1445
Fax: +82-41-660-1445
E-mail: cslim@hanseo.ac.kr

100 °C for 12 h, and 5 wt% $AgNO_3$ and 20 wt% synthetic zeolite-A were then added for the composition of Ag incorporated $SrWO_4$/zeolite. The sample mixtures were placed into crucibles and exposed to domestic microwaves (Samsung Electronics Corp. Korea) operating at a frequency of 2.45 GHz and a maximum out-put power of 1250 W for 10 minuites. The samples were treated with ultrasonic radiation and washed many times with distilled water and ethanol to remove the sodium chloride reaction by-product. The samples were dried at 100 °C in an oven. Heat-treatment of the samples was performed at 600 °C for 3 h.

The microstructure and surface morphology of the synthesized Ag incorporated $SrWO_4$/zeolite composites were observed by SEM (JSM-5600, JEOL, Japan) and EDS. FTIR (Nicolet IR 200, Thermo Electron Corporation, USA) was used to examine the thermal-decomposition behavior of the microwave-assisted SSM reaction and heat-treated Ag incorporated $SrWO_4$/zeolite composites over the frequency range, 400 °C to 4000 cm^{-1}. The PL spectra were recorded using a spectrophotometer (Perkin Elmer LS55, UK) at room temperature. Raman spectroscopy measurements were performed using LabRam HR (Jobin-Yvon, France). The 514.5 nm line of an Ar-ion laser was used as excitation source, the power was kept at 0.5 mW on the samples.

Results and Discussion

Fig. 1 shows SEM images of the Ag incorporated $SrWO_4$/zeolite composite after (a) microwave-assisted SSM reaction and (b) heat-treatment at 600 °C for 3 h. The sample mixture synthesized by the microwave-assisted SSM reaction is observed in Fig. 1(a). The samples were treated with ultrasonic radiation, washed many times and heat-treated at 600 °C for 3 h. The composite after heat-treatment at 600 °C for 3 h resulted in a homogeneous morphology with particle sizes of 3-5 μm in Fig. 1(b). The spherical small particles of silver were well immobilized in the porous $SrWO_4$/zeolite matrix. The Ag incorporated

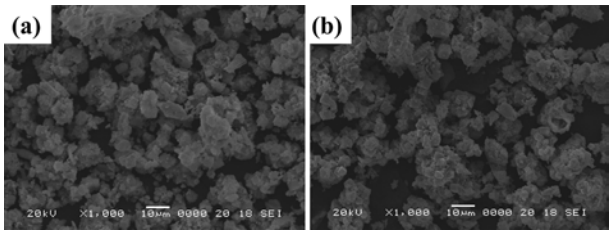

Fig. 1. SEM images of Ag incorporated $SrWO_4$/zeolite composite after (a) the microwave-assisted SSM reaction and (b) heat-treatment at 600 °C for 3 h.

$SrWO_4$/zeolite composites were well synthesized in a green manner without the generation of solvent waste, because the microwave radiation provided the energy required to overcome the energy barrier. It helped to heat the bulk of the material uniformly resulting in fine particles with a controlled morphology, and to fabricate the product in a green manner without the generation of solvent waste. The SSM reaction, such as $SrCl_2 + Na_2WO_4 \rightarrow SrWO_4 + 2NaCl$, involves the exchange of atomic/ionic species, where the driving force is the exothermic reaction with a high lattice energy accompanying the formation of NaCl [13, 14]. SSM reactions occur so rapidly that the exothermic reaction is essentially used to heat up the solid products. The SSM reaction provides a convenient route for the synthesis of the Ag incorporated $SrWO_4$/zeolite composite, which were obtained in the form of loosely connected micrometer-sized particles at considerably lower temperatures than those usually employed for their synthesis. For the Ag incorporated $SrWO_4$/zeolite composite materials to be used for practical applications, control of the particle size distribution and morphology of the particles is needed. The well-defined features of the Ag incorporated $SrWO_4$/zeolite composite synthesized by microwave-assisted SSM reactions have a control over the morphology of the final particles, and can be used for technological applications. Fig. 2 shows EDS patterns (a), qualitative compositions

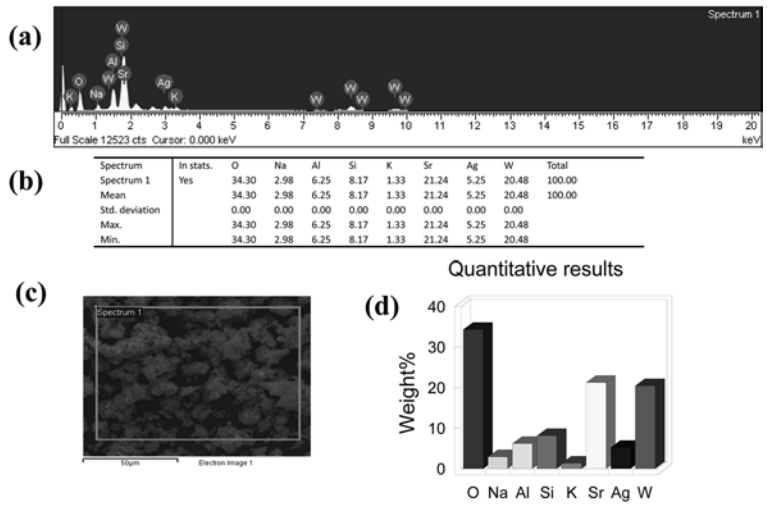

Fig. 2. EDS patterns (a), qualitative compositions (b), a SEM image (c) and qualitative results (d) of the synthesized Ag incorporated $SrWO_4$/zeolite composite.

(b), a SEM image (c) and qualitative results (d) of the synthesized Ag incorporated $SrWO_4$/zeolite composite. The EDS patterns and qualitative compositions in Fig. 2(a, b) could be assigned to the Ag-$SrWO_4$/zeolite-A composite. This means that the Ag incorporated $SrWO_4$/zeolite composite can be successfully synthesized using this SSM reaction assisted by a microwave irradiation. The crystals of $SrWO_4$ were primarily co-mixed with porous zeolite-A. The qualitative results of the morphology in Fig. 2(c, d) were composed of Ag, $SrWO_4$ and zeolite-A.

Fig. 3 shows FTIR spectrum of the Ag incorporated $SrWO_4$/zeolite composite at the wavenumber range of 480-4000 cm^{-1}. The stretching vibration was detected as a strong W-O stretch in the $[WO_4]^{2-}$ tetrahedra at 823 cm^{-1}. Similar characteristics absorption bands of MWO_4 (M = Ba, Ca, Sr) for the scheelite oxides having S_4 site symmetry in this region have been reported in the literature [6]. The $[WO_4]^{2-}$ is constituted by four internal modes ($\nu_1(A_1)$, $\nu_2(E)$, $\nu_3(F_2)$ and ν_4 (F_2)) specified as symmetric stretching, symmetric bending, asymmetric sytreching and asymmetric bending modes [12]. All these modes are Raman active, whereas only $\nu_3(F_2)$ and ν_4 (F_2) are IR active.

Fig. 4 presents the PL emission spectrum of the Ag incorporated $SrWO_4$/zeolite composite by microwave-assisted SSM synthesis and heat-treatment at 600 °C for 3 h. It is generally assumed that the measured emission spectra of metal tungstates are mainly attributed to the charge-transfer transitions within the $[WO_4]^{2-}$ complex [15, 16]. With excitation at 250 nm, the spectra show rugged peaks, which are composed of three types of groups. The first major peaks are located at the blue wavelength 425-450 nm, the second neighbored shoulders at 460-490 and the third sloped shoulders at 530-550 nm. The emission spectrum of 4-8 narrow neighbored and sloped shoulders, namely the spread-eagle-shape, at approximately 460-550 nm are considered to form from defect structures [17]. Generally, the presence of Gaussian components indicates that the electronic levels corresponding to relaxed excited state of an emission center belong to a degenerate

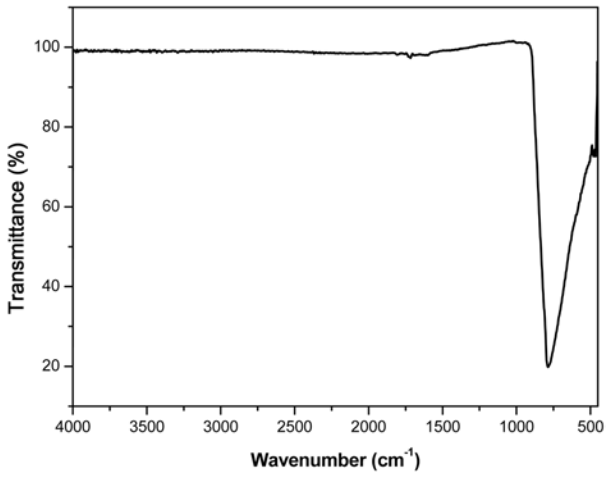

Fig. 3. FT-IR spectrum of the Ag incorporated $SrWO_4$/zeolite composite.

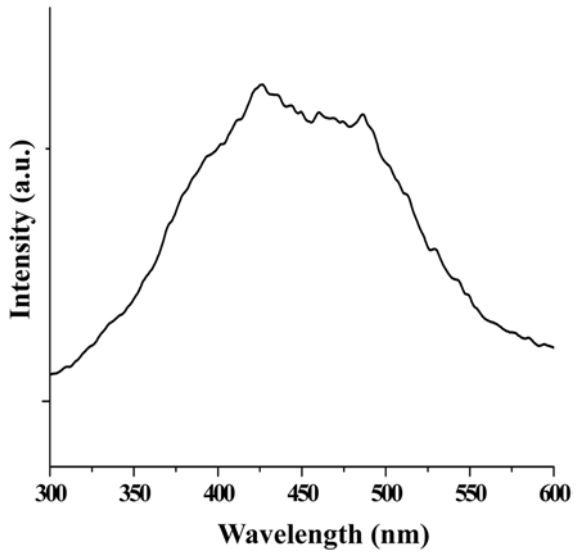

Fig. 4. PL emission spectrum of the Ag incorporated $SrWO_4$/zeolite composite exited at 250 nm.

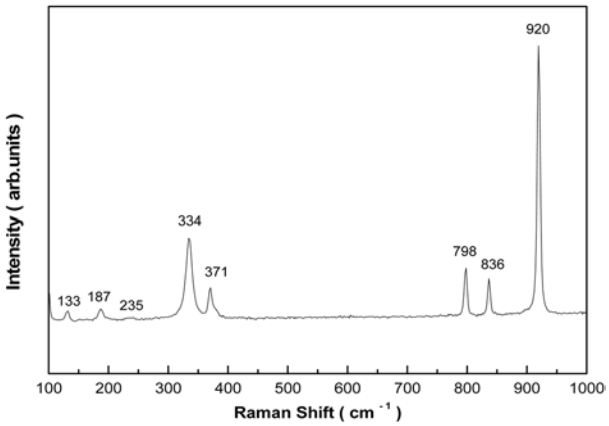

Fig. 5. Raman spectrum of the Ag incorporated $SrWO_4$/zeolite composite excited by the 514.5 nm line of an Ar-ion laser at 0.5 mW on the samples.

excited state influenced by some perturbation, e.g. a local low symmetry crystal field [18]. Such emission peaks can be explained by the influence of the Jahn-Teller effect [19] on the degenerated excited state of $[WO_4]^{2-}$ tetrahedron.

Fig. 5 shows a Raman spectrum of the Ag incorporated $SrWO_4$/zeolite composite excited by the 514.5 nm line of an Ar-ion laser kept at a power of 0.5 mW on the samples. The vibration modes in the Raman spectrum of the Ag incorporated $SrWO_4$/zeolite composite are classified into two groups, internal and external [20]. The internal vibrations are related to the $[WO_4]^{2-}$ molecular group with a stationary mass center. The external vibrations or lattice phonons are associated with the motion of the Sr^{2+} cation and rigid molecular units. In the free space, $[WO_4]^{2-}$ tetrahedra show T_d-symmetry. The Raman modes for the Ag-$SrWO_4$/zeolite-A composite in Fig. 5 were detected as $\nu_1(A_g)$, $\nu_3(B_g)$, $\nu_3(E_g)$, $\nu_4(E_g)$, $\nu_4(B_g)$ and $\nu_2(B_g)$ vibrations at 920, 836, 798, 371, 334 and 235 cm^{-1}, respectively, which provide evidence of a scheelite structure. The well-resolved

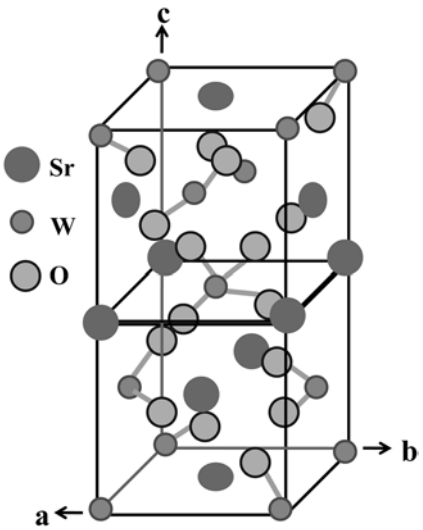

Fig. 6. Unit cell of the $SrWO_4$ scheelite-type structure with the space group $I\,4_1/a$. Sr, O and W atoms are represented by large, medium and small spheres.

sharp peaks for the Ag-$SrWO_4$/zeolite-A composite indicate that the synthesized particles are highly crystallized. A free rotation mode was detected at 187 cm^{-1} and external modes were localized at 133 cm^{-1}. This result is in agreement with that reported in the literature [13]. The internal vibration mode frequencies exhibited a dependence on the lattice parameters and the degree of the partially covalent bond between the cation and molecular ionic group $[WO_4]^{2-}$. The type of cations (Ca^{2+}, Sr^{2+}, Ba^{2+}) can influence the Raman modes by changing the size of the crystal unit cell and by a covalent cation effect [20].

Fig. 6 shows the unit cell of the $SrWO_4$ scheelite-type structure with the space group $I\,4_1/a$. Metal tungstates with large bivalent cations (e.g., Ca, Ba, Pb, and Sr) tend to have a scheelite-type tetragonal structure, whereas small cationic radii (e.g., Zn, Fe, Mn, Co, and Ni) favor the formation of a wolframite-type monoclinic structure. The main difference between the above two structures is that each W atom is surrounded by four O atoms in a scheelite-type structure, whereas the wolframite-type structure contains six O atoms surrounding each W atom. The Sr and W sites in Fig. 6 present S_4 point symmetry. The unit cell of $SrWO_4$ presents the W atoms surrounded by four O atoms in a tetragonal configuration and the Sr atoms surrounded by eight O atoms.

Conclusions

An Ag incorporated $SrWO_4$/zeolite composite was successfully synthesized by the SSM route with a microwave irradiation, showing a well immobilized morphology with particle sizes of 3-5 μm. The stretching vibration in FTIR was detected as a strong W-O stretch in the $[WO_4]^{2-}$ tetrahedra at 823 cm^{-1}. With excitation at 250 nm, the major peaks of PL are located at the blue wavelength of 425-450 nm. The emission spectrum of 4-8 narrow neighbored and sloped shoulders were considered to form from defect structures, which was explained by the influence of the Jahn-Teller effect. The well-resolved Raman spectrum for the Ag incorporated $SrWO_4$/zeolite composite at 920, 836, 798, 371, 334 and 235 cm^{-1} provide evidence of a scheelite structure. A free rotation mode was detected at 187 cm^{-1} and the external modes were localized at 133 cm^{-1}.

Acknowledgement

This study was supported by Basic Science Research Program through the National Research Foundation of Korea (NRF) funded by the Ministry of Education, Science and Technology (2010-0023911).

References

1. Z. Shan, Y. Wang, H. Ding and F. Huang, J. Mol. Cat. A: Chemical 302 (2009) 54-58.
2. G. Zhang, S. Yang, Z. Li, L. Zhang, W. Zhou, H. Zhang, H. Shen and Y. Wang, Applied Surface Science, 257 (2010) 302-305.
3. T. Thongtem, S. Kungwankunakorn, B. Kuntalue, A. Phuruangrat and S. Thongtem, J. Alloys Compd. 506 (2010) 475-481.
4. A.J. Rondinone, M. Pawel, D. Travaglini, S. Mahurin and S. Dai, J. Coll. Inter. Sci. 306 (2007) 281-284.
5. S. Thongtem, S. Wannapop and T. Thongtem, Trans. Nonferr.China 19 (2009) s100-s104.
6. G. Zhang, R. Jia and Q. Wu, Mat. Sci. Eng. B 128 (2006) 254-259.
7. R. Dinesh, T. Fujiwara, T. Watanabe, K. Byrappa and M. Yoshimura, J. Mat. Sci. 41 (2005) 1541-1546.
8. K. Lennstrom, S.J. Limmer and G. Cao, Thin Solid Films 434 (2003) 55-61.
9. D. Rangappa, T. Fujiwara, T. Watanabe and M. Yoshimura, J. Electroceram. 17 (2006) 853-860.
10. Y. Wang, J. Ma, J. Tao, X. Zhu, J. Zhou, Z. Zhao, L. Xie and H. Tian, Mat. Lett. 60 (2006) 291-293.
11. L. Zhang, C. Lu, Y. Wang and Y. Cheng, Mat. Chem. Phys. 103 (2007) 433-436.
12. J.T. Kloprogge, M.L. Weier, L.V. Duong and R.L. Frost, Mat. Chem. Phys. 88 (2004) 438-443.
13. P. Parhi, T.N. Karthik and V. Manivannan, J. Alloys Compd. 465 (2008) 380-386.
14. V. Thangadurai, C. Knittlmayer and W. Weppner, Mat. Sci. Eng. B 106 (2004) 228-233.
15. D.A. Spassky, S.N. Ivanov, V.N. Kolobanov, V.V. Mikhailin, V.N. Zemskov, B.I. Zadneprovski and L.I. Potkin, Radiat. Meas. 38 (2004) 607-610.
16. G.Y. Hong, B.S. Jeon, Y.K. Yoo and J.S. Yoo, J. Electrochem. Soc. 148 (2001) H161-H166.
17. M. Nikl, P. Bohacek, E. Mihokova, M. Kobayasshi, M. Ishii, Y. Usuki, V. Babin, A. Stolovich, S. Zazubovich and M. Bacci, J. Lumin. 87-89 (2000) 1136-1139.
18. K. Polak, M. Nikl, K. Nitsch, M. Kobayashi, M. Ishii, Y. Usuki and O. Jarolimek, J. Lum. 72-74 (1997) 781-783.
19. J.V. Tol and J.H. Van Der Waals, Mol. Phys. 88 (1996) 803-820.
20. T.T. Basiev, A.A. Sobol, Y.K. Voronko and P.G. Zverev, Opt. Mat. 15 (2000) 205-216.